DEEP LEARNING FOR RADAR TARGET DETECTION IN NON-HOMOGENEOUS CLUTTER

Tristan S.W. Stevens *Recep F. Tigrek* *Ruud J.G. van Sloun*

Department of Electrical Engineering, Eindhoven University of Technology, The Netherlands

ABSTRACT

Constant false alarm rate (CFAR) detectors are widely used in radar systems for detecting target returns against a background with thermal noise, clutter and interference. Many different adaptive CFAR detector schemes are already in use, however none prove to be optimal considering the presence of non-homogeneous background environments. This paper proposes an alternative detector scheme through deep learning, showing that a deep unfolded model-based network architecture significantly outperforms conventional cell averaging (CA) CFAR, as well as standard deep convolutional networks, under challenging clutter and interference conditions.

Index Terms— Radar, CNN, CFAR, Unfolding, Deep learning, Sparse decoding

1. INTRODUCTION

Constant false alarm rate (CFAR) detectors are used in radar systems and are designed to achieve high correct detection (with constant false alarm) rate in sub-optimal environments. Specifically, in the cases where the noise power is unknown and has to be estimated from the received signal, adaptive CFAR is used to establish a local threshold. One of the more conventional detectors is a cell averaging (CA) CFAR detector, which determines its threshold by evaluating the neighbouring cells of the cell under test (CUT). CA CFAR assumes a homogeneous background which is a condition that is often not realizable in real world problems, suffering from performance degradation when operating in a non-homogeneous environment [1]. The unwanted radar returns that form the basis of this environment are known as clutter.

Earliest research considers more general formulations of the problem of detecting signals in non-Gaussian distributions [2] and non-stationary environments [3]. Another early work on the problem of target detection in clutter focuses on the detection of target trajectory over multiple scans [4], whereas detection through a single scan is the focus of the current paper. Numerous other studies on the utilization of neural networks (NN) in radar applications for target detection in clutter environments have been conducted [5][6][7][8][9][10]. The previous research results either do not consider a non-homogeneous background or construct a different implementation of the neural network. Other works on the topic propose the use of neural networks to identify homogeneity of the background and select between CA-CFAR and OS-CFAR [11][12][13]. The neural network is not the detector in these studies.

Today, deep learning has been revolutionizing many fields of research. Motivated by the deep-learning promise, we here propose to leverage deep networks as stand-alone radar detectors that are designed to reduce the probability of false alarm in the presence of non-homogeneous clutter. We design a detailed clutter model that replicates the clutter edges, closely spaced targets and interference that form the basis of the inconsistent background that is subject to the detector. A comparison is made between the conventional CA CFAR detector, a standard convolutional neural network radar detector, and a dedicated deep unfolded model-based network. Synthetic radar data, based on the aforementioned clutter model, is used to train the deep networks as well as test the performance of the detectors.

2. SIGNAL PROCESSING

Frequency-modulated continuous-wave (FMCW) radar technology is used to measure the range and speed of a certain target, while ensuring good localization and resolution. This method uses a burst of very short chirps that ramp up in frequency. The transmitted signal is given by

$$s_{T_X}(t) = \sum_{n=0}^{N} \cos\left(2\pi\{f_c(t_n + nT_{chirp}) + \frac{\beta t_n^2}{2}\} + \varphi_0\right), \tag{1}$$

where N equals the number of pulses, f_c is the carrier frequency, T_{chirp} denotes the duration of the FMCW sweep, β is the ramp of the sweep and ϕ_0 is the initial phase. For N pulses $t = t_n + nT_{chirp}$. The received signal or "echo" s_{R_X} is a reflected and time-delayed replica of the transmitted signal with attenuation factor A. In order

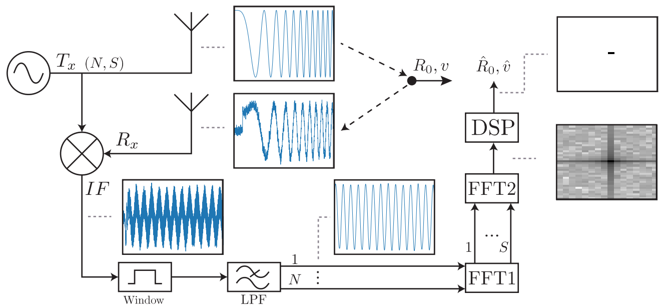

Fig. 1. Schematic overview of the complete signal processing chain. N chirps of length S are transmitted and received by the radar. The resulting Doppler image is of size (N, S). The point target attributes, $\hat{R}_0$ and $\hat{v}$ are the estimated target location and speed respectively.

to extract the range and speed information from the received signal, a mixing technique know as deramping or dechirping is performed. The resulting signal is the output of a frequency mixer with s_{T_X} and s_{R_X} as inputs. The deramped signal s_{IF} is given by the product of the s_{T_X} and s_{R_X} and analytically calculated as

$$\begin{aligned} s_{IF}(t) &= s_{T_X}(t) \cdot s_{R_X}(t) \qquad (2) \\ &\simeq \frac{A}{2} \sum_{n=0}^{N} \cos\left(2\pi[\underbrace{\frac{2\beta R_0}{c}}_{f_b} t_n + \underbrace{\frac{2 f_c v}{c}}_{f_d} nT + \underbrace{\frac{2 f_c R_0}{c}}_{\varphi}]\right), \end{aligned}$$

where R_0 is the initial location of the target, v is its speed and c denotes the speed of the FMCW signal. Both range and speed can be determined by f_b and f_d respectively. A full range-Doppler image is constructed with use of the two dimensional FFT. A complete overview of these processing steps is given in Fig. 1.

3. ENVIRONMENT MODELS

The CFAR detector used in conventional radar systems is based on binary hypothesis testing under a specific distribution. If the distribution is homogeneous across the entire range, a fixed-threshold CFAR detector can be utilized. However, when the distribution of the signal processing output for the null hypothesis is range-dependent, a CFAR detector with a fixed detection threshold is bound to under-perform.

To evaluate the performance of the proposed deep-learning-based radar detector against a conventional CFAR solution to this problem (i.e. cell-averaging CFAR), we simulate three scenarios that deviate from the homogeneous distribution assumption. The first scenario involves detection of multiple targets. In this case, the energy from each target leaks to adjacent range and Doppler resolution cells, which are termed sidelobes of a target. As a result, a target with large radar cross section (RCS) may shadow another target with smaller RCS. Moreover, the tatistics of the neighboring resolution cells will be altered, which may in turn give rise to increased false alarm rate or reduced probability of detection.

The second scenario concerns the presence of an interfering signal. When the interfering signal is from another FMCW radar that operates in the same frequency band, 'ghost targets' will appear on the range-Doppler output of the victim radar [14]. This effect cannot be accounted for by standard CFAR detectors, but has to be dealt with by tracking algorithms over several measurements. To account for other interference effects that can be modelled as stochastic processes, it is assumed that an interfering source produces an effect that appears as noise confined between certain range intervals. The increased noise causes edges inside the Doppler image and can conceal target returns, respectively resulting in higher probabilities of false alarm and lower probabilities of detection.

The third scenario is detection of targets in non-homogeneous clutter environment. Clutter is defined as the accumulation of all unwanted echoes that do not originate from a target. Targets of interest are often differentiated from clutter according to their velocity: Clutter is assumed to have zero velocity while targets of interest are assumed moving. Pulse Doppler radars measure the velocity of each target from the Doppler effect described in (2). The clutter model implemented in the simulator consists of placing a contiguous clutter area between certain ranges to generate the non-homogeneous environment. Internal clutter motion is modeled as fluctuations in the clutter RCS from one FMCW pulse to the next [15]. Such internal clutter motion gives rise to a Doppler spectrum which not only has the DC component associated with the stationary reflectors, but also components at higher Doppler frequencies. Models as well as experimental results from previous literature are used as a ground rule for recreating the spectral shape of the most common clutter types [16] [17] [18].

4. CELL AVERAGING CFAR DETECTOR

In order to detect targets, cell averaging CFAR detectors use a local threshold, determined by the noise statistics. Each cell under test (CUT) is evaluated and compared with the threshold T to determine whether a target is located in the range bin of the CUT. The threshold is derived from the noise power $P_n = \frac{1}{N}\sum_{i=1}^{N}(\mathrm{TC})_i$, where TC is a training or reference cell and N the number of these cells. Noise statistics are solely derived from the surrounding training cells. In order to satisfy a constant probability of false alarm P_{fa}, a constant scale factor α

is multiplied with the estimated noise power [1] resulting in the threshold value $T = \alpha P_n$.

The reference cells are not located directly adjacent to the CUT. Instead some guard cells (GC) are inserted. Guard cells are included to prevent target returns from leaking into training cells and adversely effecting the noise power estimate.

5. DEEP LEARNING BASED DETECTORS

Two different deep learning structures are discussed; a regular feed forward CNN and an unfolded iterative method. Both networks are trained under supervised learning with simulated radar images containing multiple targets in a cluttered environment. The detector outputs are subsequently processed by a centroid localization algorithm to obtain high-resolution localizations.

5.1. Convolutional network

The regular CNN consists of four hidden layers, each yielding 32 new feature-map representations through a set of 3×3 convolutional kernels, followed by ReLU activations. A final layer then maps these 32 feature maps to a single output for every pixel/cell, indicating the probability of a target being present in such a cell. In total, the network has $28,097$ trainable parameters.

5.2. Deep unfolded ISTA

Deep unfolding methods leverage signal models to dictate an appropriate neural network architecture, and have been introduced in applications spanning from image denoising, to super-resolution imaging and clutter suppression [19][20]. We here adopt the following approximate signal model:

$$\mathbf{x} = \mathbf{A}\mathbf{z} + \mathbf{n}, \tag{3}$$

where $\mathbf{x}$, $\mathbf{z}$, and $\mathbf{n}$ are the vectorized range-Doppler measurements, underlying targets, and residual noise sources, respectively. $\mathbf{A}$ is a matrix that maps the target locations (encoded on a grid) to range-Doppler measurements. Assuming that the targets are sparsely distributed across the range-Doppler cells, Equation (3) can be solved for $\mathbf{z}$ through sparse coding, e.g. by the iterative shrinkage and thresholding algorithm (ISTA):

$$\mathbf{z}^{k+1} = \mathcal{T}_\lambda \left(\mathbf{z}^k - \mu \mathbf{A}^T \left(\mathbf{A}\mathbf{z}^k - \mathbf{x} \right) \right), \tag{4}$$

where μ determines the step size, and $\mathcal{T}_\lambda(\mathbf{z})_i = (|x_i| - \lambda)_+ \mathrm{sgn}(z_i)$ is the proximal operator of the ℓ_1 norm. Equation (4) is compactly written as:

$$\mathbf{z}^{k+1} = \mathcal{T}_\lambda \left(\mathbf{W}_1 \mathbf{x} + \mathbf{W}_2 \mathbf{z}^k \right), \tag{5}$$

with $\mathbf{W}_1 = \mu \mathbf{A}^T$, and $\mathbf{W}_2 = \mathbf{I} - \mu \mathbf{A}^T \mathbf{A}$. This recurrent structure is then unfolded into a K-layer feedforward neural network, with each layer consisting of trainable convolutions $\mathbf{W}_1^k$ and $\mathbf{W}_2^k$, along with a trainable shrinkage parameter λ^k. We here adopt a 10-layer network, i.e. $K = 10$. Notably, the resulting network only has 986 trainable parameters.

5.3. Training strategy

We train the networks through the following loss function $L(\mathbf{X}, \mathbf{Y}|\theta)$ is defined as [21]:

$$L(\mathbf{X}, \mathbf{Y}|\theta) = ||g(\sigma) * \mathbf{Y} - f_\theta(\mathbf{X})||_2^2 + \lambda ||f_\theta(\mathbf{X})||_1 \tag{6}$$

where $g(\sigma)$ is a Gaussian kernel with standard deviation σ, $\mathbf{Y}$ the binary target map, and $f_\theta(\mathbf{X})$ the predictions of a network parameterized by θ. The first term of (6) pushes the network predictions close to the smoothed targets, while the second promotes sparsity of predictions through an ℓ_1 norm with weight λ. During training we use an annealing scheme for σ, starting with a relatively high value ($\sigma = 10$), and reducing it every epoch until reaching a set minimum value ($\sigma = 0.2$). In practice, this annealing approach led to more stable training.

6. DATA SETS AND METRICS

The performance of the radar detectors is evaluated on four datasets, all composed of full-size range-Doppler images with corresponding labels (binary images) containing the targets positions. The images are constructed by means of the FMCW signal processing and environment model, previously described in Sections 2 and 3. The first dataset comprises images with single-target returns. This data set is used as a reference, since it is expected the detectors have no problem detecting the targets when the images are free of unwanted echoes. The second dataset contains range-Doppler images with multiple targets that have a high probability of being closely spaced. The third dataset contains clutter in addition to multiple targets. The last dataset includes multiple targets as well as interference.

We use three metrics to evaluate the detector performance on these datasets, recall, precision, and error, which we define as follows. The recall represents the percentage of correctly identified targets, with a target regarded as correctly identified whenever it is found within the vicinity (radius = 6 px) of the actual target. The precision then covers the amount of false alarms, and lastly, the distance from each prediction to the closest label is calculated (localization error).

Table 1. Quantitative results of the implemented detectors.

Detector	CA CFAR			Standard CNN			Deep unfolded ISTA		
Data set	Error($\mu \pm \sigma$)	Recall	Precis.	Error($\mu \pm \sigma$)	Recall	Precis.	Error($\mu \pm \sigma$)	Recall	Precis.
single	0.30 ± 0.20	0.98	0.89	0.35 ± 0.24	1.00	1.00	0.35 ± 0.24	1.00	1.00
multiple	0.94 ± 2.14	0.82	0.98	0.41 ± 0.31	1.00	1.00	0.38 ± 0.37	0.99	1.00
interfer.	1.03 ± 2.47	0.71	0.79	0.42 ± 0.43	0.98	1.00	0.42 ± 0.43	0.99	0.99
clutter	1.12 ± 3.20	0.74	0.31	0.50 ± 0.72	0.97	0.82	0.46 ± 0.56	0.98	0.93

7. RESULTS

Table 1 shows quantitative results of the detectors. As expected, all three detectors perform well for the localization of single targets in a homogeneous environment. When evaluating all detectors with the multiple-target dataset we observe that CA CFAR is not able to recognize all of the closely spaced targets. Indeed, the weaker reflection of the adjacent target is often masked by the side lobes of the stronger target, raising the threshold T and resulting in a missed detection. In contrast, both deep learning implementations do not suffer from this, only leading to a slight increase in localization error. In the event of interference, a more significant difference in performance is observed between detectors. The CA CFAR detector seems to perform worse especially in cases where the targets are located on the edge of interference, of which and example is depicted in Fig. 2. Both deep learning detectors again perform similarly well in this scenario. From Table 1 we observe that clutter has the strongest impact on detection performance. Notably, the deep unfolded ISTA network outperforms both other methods in this case.

A 2D range-Doppler image containing both interference and clutter is shown in Fig. 3, along with the corresponding detections by CA CFAR and the deep learning methods. The former is only able to detect half of the targets and is again outperformed by the CNN and unfolded ISTA network.

8. CONCLUSIONS

In this paper we proposed two radar detectors based on deep learning. We showed that these detectors are able to localize targets across challenging conditions and environments (containing clutter, interference and closely spaced targets), thereby outperforming the conventional cell-averaging CFAR detector. In addition, we demonstrated that a compact (< 1000 parameters) model-based deep unfolded network is up to par with a more complex convolutional network, and even outperforms it for the most challenging range-Doppler spectra containing strong clutter. Although the results presented in this work show promise, validation on real radar data is needed, and will be part of future work.

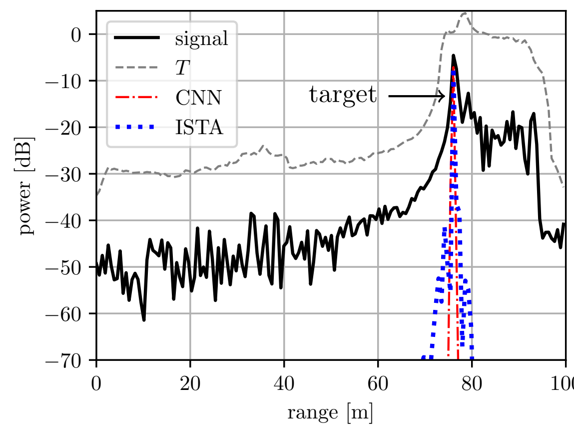

Fig. 2. Signal with interference and a target located near the edge. The CA CFAR detector misses the target due to the presence of the interference. The deep learning methods are able to locate the target correctly.

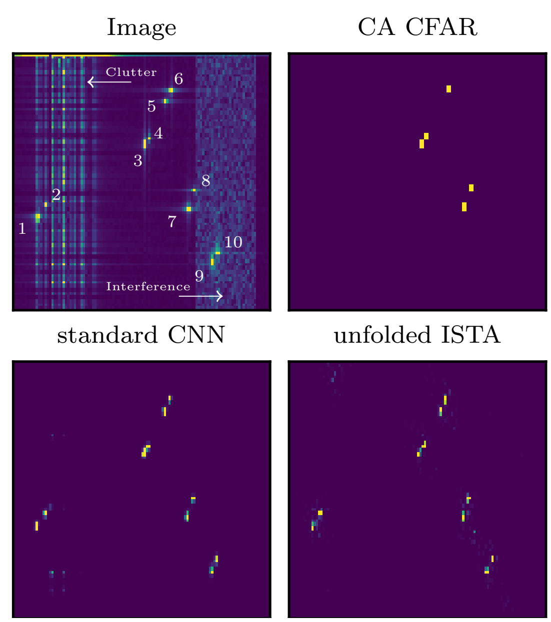

Fig. 3. Visual comparison of the performance of the radar detectors when subjected to clutter (left), interference (right) and multiple targets (1-10).

9. REFERENCES

[1] Prashant P Gandhi and Saleem A Kassam, "Analysis of cfar processors in nonhomogeneous background," *IEEE Transactions on Aerospace and Electronic systems*, vol. 24, no. 4, pp. 427–445, 1988.

[2] Prashant P Gandhi and Viswanath Ramamurti, "Neural networks for signal detection in non-gaussian noise," *IEEE Transactions on signal processing*, vol. 45, no. 11, pp. 2846–2851, 1997.

[3] Simon Haykin and Tarun Kumar Bhattacharya, "Modular learning strategy for signal detection in a nonstationary environment," in *MILCOM 97 MILCOM 97 Proceedings*. IEEE, 1997, vol. 3, pp. 1113–1116.

[4] Michael W Roth, "Neural networks for extraction of weak targets in high clutter environments," *IEEE Transactions on Systems, Man, and Cybernetics*, vol. 19, no. 5, pp. 1210–1217, 1989.

[5] Farid Amoozegar and Malur K Sundareshan, "A robust neural network scheme for constant false alarm rate processing for target detection in clutter environment," in *Proceedings of 1994 American Control Conference*. IEEE, 1994, vol. 2, pp. 1727–1728.

[6] Diego Andina and José L Sanz-González, "Application of a neural network to radar detection," in *Proc. Of European Conference on Circuit Theory and Design*, 1995, pp. 573–576.

[7] Gustavo López-Risueño, Jesús Grajal, Simon Haykin, and Rosa Díaz-Oliver, "Convolutional neural networks for radar detection," in *International Conference on Artificial Neural Networks*. Springer, 2002, pp. 1150–1155.

[8] Dilip Gopichand Khairnar, SN Merchant, and Uday B Desai, "Radar signal detection in non-gaussian noise using rbf neural network.," *JCP*, vol. 3, no. 1, pp. 32–39, 2008.

[9] A Lotfi, K Mezzoug, and A Benyettou, "Rotated kernel neural networks for radar target detection in background noise," *Journal of Applied Sciences (Faisalabad)*, vol. 10, no. 13, pp. 1331–1335, 2010.

[10] Gustavo Lopez-Risueno, Jesus Grajal, and Rosa Diaz-Oliver, "Target detection in sea clutter using convolutional neural networks," in *Proceedings of the 2003 IEEE Radar Conference*. IEEE, 2003, pp. 321–328.

[11] Budiman PA Rohman, Dayat Kurniawan, and M Tajul Miftahushudur, "Switching ca/os cfar using neural network for radar target detection in non-homogeneous environment," in *2015 International Electronics Symposium (IES)*. IEEE, 2015, pp. 280–283.

[12] NB Gálvez, JE Cousseau, JL Pasciaroni, and OE Agamennoni, "Improved neural network based cfar detection for non homogeneous background and multiple target situations," *Latin American applied research*, vol. 42, no. 4, pp. 343–350, 2012.

[13] NB Gálvez, JE Cousseau, JL Pasciaroni, and OE Agamennoni, "Efficient non homogeneous cfar processing," *Latin American applied research*, vol. 41, no. 1, pp. 1, 2011.

[14] Thayananthan Thayaparan, M Daković, and L Stanković, "Mutual interference and low probability of interception capabilities of noise radar," *IET Radar, Sonar & Navigation*, vol. 2, no. 4, pp. 294–305, 2008.

[15] Güneş Tanriverdi, *Arma Model Based Clutter Estimation and its Effect on Clutter Supression Algorithms*, Ph.D. thesis, Middle East Technical University, 2012.

[16] P Lombardo and JB Billingsley, "A new model for the doppler spectrum of windblown radar ground clutter," in *Proceedings of the 1999 IEEE Radar Conference. Radar into the Next Millennium*. IEEE, 1999, pp. 142–147.

[17] B Billingsley, A Farina, Fulvio Gini, MV Greco, and P Lombardo, "Impact of experimentally measured doppler spectrum of ground clutter on mti and stap," *Radar 97*, 1997.

[18] David A Shnidman, "Generalized radar clutter model," *IEEE Transactions on Aerospace and Electronic Systems*, vol. 35, no. 3, pp. 857–865, 1999.

[19] Karol Gregor and Yann LeCun, "Learning fast approximations of sparse coding," in *Proceedings of the 27th International Conference on International Conference on Machine Learning*. Omnipress, 2010, pp. 399–406.

[20] Oren Solomon, Regev Cohen, Yi Zhang, Yi Yang, Qiong He, Jianwen Luo, Ruud JG van Sloun, and Yonina C Eldar, "Deep unfolded robust pca with application to clutter suppression in ultrasound," *IEEE transactions on medical imaging*, 2019.

[21] Ruud JG van Sloun, Regev Cohen, and Yonina C Eldar, "Deep learning in ultrasound imaging," *Proceedings of the IEEE*, 2019.